High temperature phase transitions in synthetic RbGaSi2O6 and RbFeSi2O6 leucite analogues

BELL, Anthony

High temperature phase transitions in synthetic $RbGaSi_2O_6$ and $RbFeSi_2O_6$ leucite analogues.

Sheffield Hallam University | Materials and Engineering Research Institute

A.M.T.Bell (Anthony.Bell@shu.ac.uk)

Introduction

Leucite ($KAlSi_2O_6$) [1] is a tetrahedrally coordinated silicate framework mineral. Synthetic analogues of leucite can be synthesised with stoichiometries of $A^+_2B^{2+}Si_5O_{12}$ or $A^+C^{3+}Si_2O_6$, with some of the silicon framework cations partially replaced by divalent (*B*) or trivalent (*C*) cations. A monovalent extraframework alkali metal (*A*) cation is also incorporated in these structures to balance the charges. Ambient temperature structures of synthetic anhydrous leucite analogues (where *A* = K or Rb and *C* = Al, Ga or Fe) all have $I4_1/a$ tetragonal structures [1-5] with **disordered** tetrahedrally coordinated sites (T-sites).

On heating these tetragonal leucites can undergo phase transitions to *Ia*-3*d* cubic. Phase transitions have been reported for $KCSi_2O_6$ [2, 4] and $RbAlSi_2O_6$ [4]. High temperature X-ray powder diffraction has been done on $RbGaSi_2O_6$ and $RbFeSi_2O_6$ leucite analogues to look for more phase transitions.

Synthesis

$RbGaSi_2O_6$ and $RbFeSi_2O_6$ were prepared from appropriate stoichiometric mixtures of Rb_2CO_3, SiO_2, and Ga_2O_3 or Fe_2O_3, each mixture was loaded into Pt crucibles. The $RbGaSi_2O_6$ mixture was heated to 1473K and the $RbFeSi_2O_6$ mixture was heated to 1673K.

Data collection and analysis

Each sample was loaded into a Pt flat plate sample holder which was inserted in an Anton Paar HTK1200N high temperature stage mounted on a PANalytical X'Pert Pro MPD. High temperature X-ray powder diffraction data, using Cu Kα X-rays and a PIXCEL-1D area detector, were collected on $RbGaSi_2O_6$ up to 973K and on $RbFeSi_2O_6$ up to 873K.

The $I4_1/a$ tetragonal structure for $RbGaSi_2O_6$ [5] was used as a starting model for Rietveld refinement, Ga_2O_3 impurity [6] was included as a second phase for Rietveld refinements [7] which were done using FULLPROF [8].

The $I4_1/a$ tetragonal structure for $RbFeSi_2O_6$ [4] was used as a starting model for Rietveld refinement. Mössbauer Spectroscopy [9] on the $RbFeSi_2O_6$ sample also showed the presence of Fe_3O_4 [10], so this was included as a second phase for Rietveld refinements which were done using GSAS-II [11].

High temperature X-ray Powder Diffraction.

Figure 1 ($RbGaSi_2O_6$) and Figure 2 ($RbFeSi_2O_6$) show how the tetragonal 004 and 400 Bragg reflections converge to a single cubic 400 reflection on heating. Rietveld refinements below the transition were done using the ambient temperature $I4_1/a$ tetragonal structures. Above the transition Rietveld refinements were done using the *Ia*-3*d* cubic structures for $CsGaSi_2O_6$ [5] and $CsFeSi_2O_6$ [3] as starting structures with Rb replacing Cs. Figure 1 shows that the $RbGaSi_2O_6$ transition takes place at 733K and Figure 2 shows that the $RbFeSi_2O_6$ transition takes place at 673K. Figure 3 shows how the lattice parameters change with temperature for both $RbGaSi_2O_6$ and $RbFeSi_2O_6$. Figures 4 and 5 show the Rietveld difference plots for $RbFeSi_2O_6$ at 603K and 773K. Figures 6 and 7 show VESTA [12] plots of crystal structures for $RbFeSi_2O_6$ at 603K and 773K, pink spheres represent Rb^+ cations, blue tetrahedra represent disordered $(Si,Fe)O_4$ units and red spheres represent O^{2-} anions.

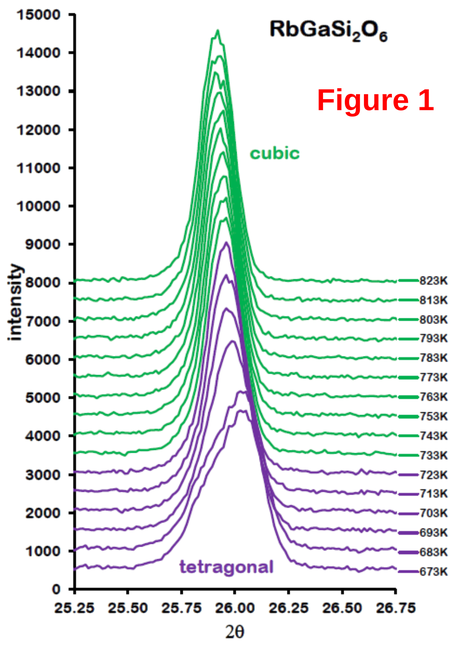

Figure 1

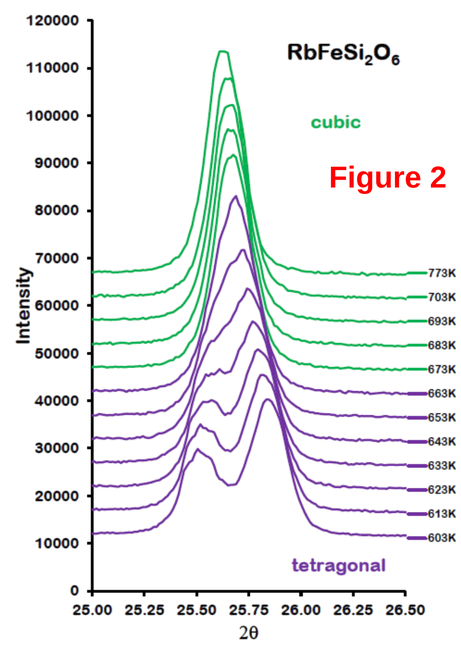

Figure 2

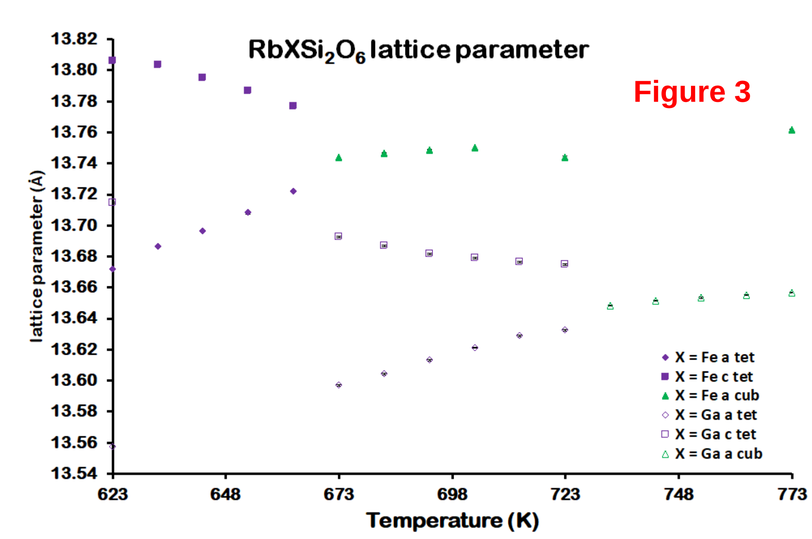

Figure 3

Figure 4

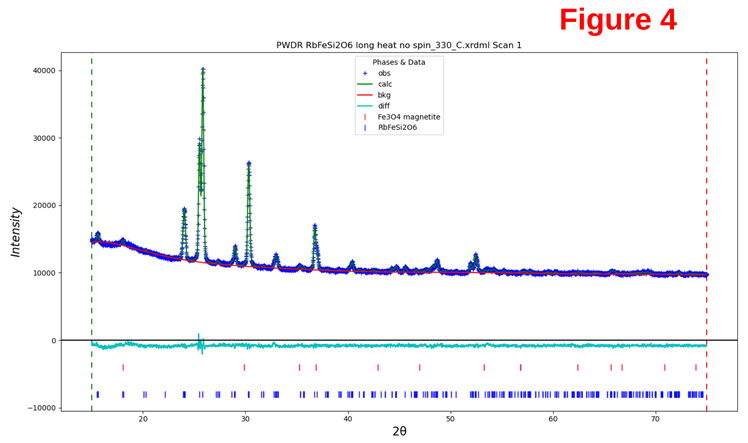

Figure 5

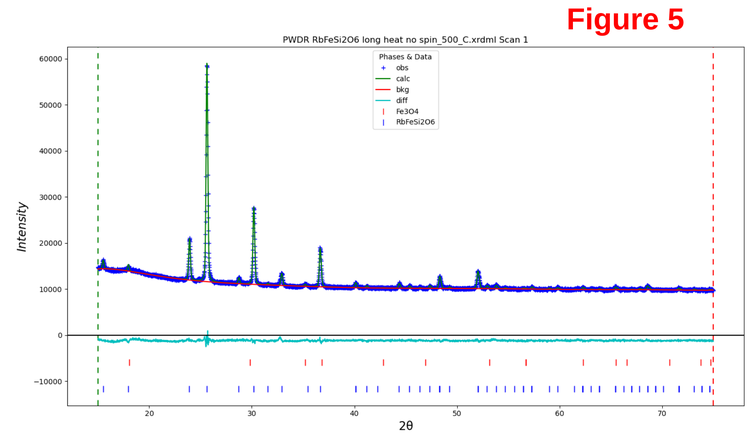

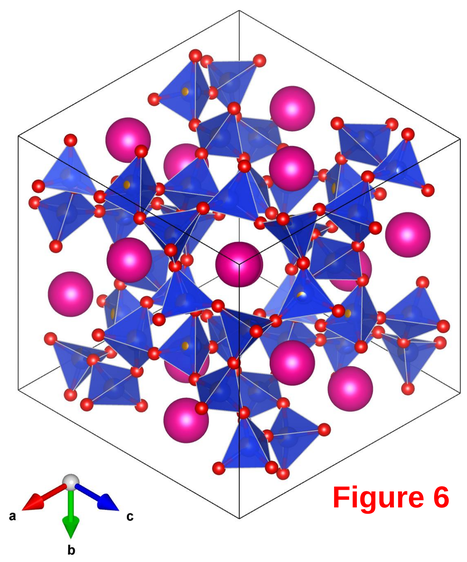

Figure 6

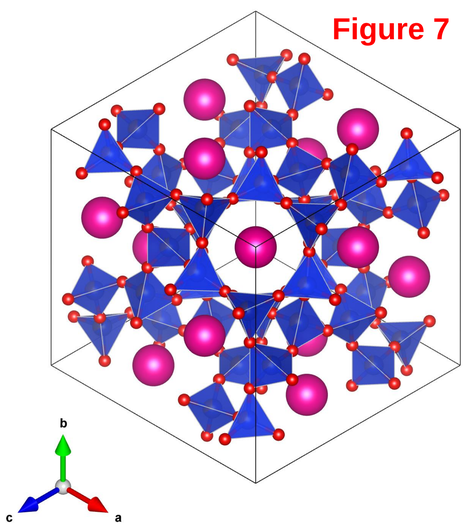

Figure 7

Table 1 - Ambient temperature lattice parameters and $I4_1/a$ tetragonal to *Ia*-3*d* cubic phase transition temperatures (T) for $A^+C^{3+}Si_2O_6$ leucite analogues.

Stoichiometry	a(Å)	c(Å)	c/a	T (K)	Reference
$KAlSi_2O_6$	13.0548(2)	13.7518(2)	1.05339(3)	943	[4]
$KGaSi_2O_6$	13.1099(4)	13.8100(4)	1.05340(6)	773-973	[2]
$KFeSi_2O_6$	13.2036(2)	13.9545(3)	1.05687(4)	853	[4]
$RbAlSi_2O_6$	13.2918(2)	13.7412(2)	1.03381(3)	753	[4]
$RbGaSi_2O_6$	13.3752(6)	13.8040(6)	1.03206(9)	733	This work
$RbFeSi_2O_6$	13.4500(15)	13.9274(7)	1.03549(17)	673	This work

Discussion

High temperature X-ray powder diffraction has been done on $RbGaSi_2O_6$ and $RbFeSi_2O_6$ leucite analogues, in both cases there are phase transitions from $I4_1/a$ tetragonal to *Ia*-3*d* cubic. Ambient temperature lattice parameters and transition temperatures are given in Table 1 for 6 different $A^+C^{3+}Si_2O_6$ leucite analogues. Figures 6 ($I4_1/a$ 603K) and 7 (*Ia*-3*d* 773K) show crystal structures for $RbFeSi_2O_6$. Note how the tetragonal framework is more collapsed [13] than the cubic framework.

Due to the smaller ionic radii [14] for K^+ compared to Rb^+ the $KCSi_2O_6$ leucite analogues have higher c/a ratios and transition temperatures than the corresponding $RbCSi_2O_6$ leucite analogues. The smaller alkali metal cation ionic radius for K^+ compared to Rb^+ means a greater framework collapse. Consequently more energy is needed to expand the framework to a less collapsed cubic structure increasing the transition temperature.

Conclusions

High temperature X-ray powder diffraction has been done on $RbGaSi_2O_6$ and $RbFeSi_2O_6$ leucite analogues. In both cases there are $I4_1/a$ tetragonal to *Ia*-3*d* cubic phase transitions. The transition temperatures are 733K ($RbGaSi_2O_6$) and 673K ($RbFeSi_2O_6$).

References:- [1] Mazzi, F., *et al*. (1976). *Am. Mineral.*, 61, 108-115. [2] Bell, A.M.T. & Henderson, C.M.B. (2020). *Journal of Solid State Chemistry*, 284, 121142. [3] Bell, A.M.T. & Henderson, C.M.B. (1994). *Acta Cryst.,* C50, 1531-1536. [4] Palmer, D.C., *et al.* (1997). *Am. Mineral.*, 82, 16-29. [5] Bell, A.M.T. & Stone A.H. (2021). *Powder Diffraction,* 36(4), 273–281. [6] da Silva, M. A. F. M., *et al*. (2012). *Journal of Physics: Conference Series 340*, 1–7. [7] Rietveld, H. M. (1969). *J. Appl. Cryst.* 2, 65–71. [8] Rodríguez-Carvajal, J. (1993). *Phys. B: Condens. Matter,* 192, 55–69. [9] Bell, A.M.T. & Scrimshire A. (2021). *In preparation.* [10] Fleet, M. E. (1981). *Acta Cryst.* B37, 917–920. [11] Toby B.H. & Von Dreele R.B. (2013). *J. Appl. Cryst.* 46, 544–549. [12] Momma, K. & Izumi, F. (2008). *J. Appl. Cryst.* 41, 653–658. [13] Taylor, D. & Henderson, C.M.B. (1968). *Am. Mineral.*, 53, 1476-1489. [14] Shannon, R. D. (1976). *Acta Cryst.* A32, 751–767.